

Search for the $X(1812)$ in $B^\pm \rightarrow K^\pm \omega \phi$

C. Liu,³⁷ Z. P. Zhang,³⁷ I. Adachi,⁹ H. Aihara,⁴³ K. Arinstein,^{1,32} T. Aushev,^{19,14} A. M. Bakich,⁴⁰ E. Barberio,²² A. Bay,¹⁹ V. Bhardwaj,³⁴ A. Bozek,²⁸ M. Bračko,^{21,15} T. E. Browder,⁸ M.-C. Chang,⁴ A. Chen,²⁵ B. G. Cheon,⁷ I.-S. Cho,⁴⁷ Y. Choi,³⁹ J. Dalseno,⁹ A. Drutskoy,² W. Dungel,¹² S. Eidelman,^{1,32} N. Gabyshev,^{1,32} P. Goldenzweig,² H. Ha,¹⁷ J. Haba,⁹ B.-Y. Han,¹⁷ K. Hayasaka,²³ M. Hazumi,⁹ Y. Hoshi,⁴² H. J. Hyun,¹⁸ K. Inami,²³ A. Ishikawa,³⁶ R. Itoh,⁹ M. Iwasaki,⁴³ Y. Iwasaki,⁹ D. H. Kah,¹⁸ J. H. Kang,⁴⁷ P. Kapusta,²⁸ N. Katayama,⁹ T. Kawasaki,³⁰ H. O. Kim,¹⁸ Y. I. Kim,¹⁸ Y. J. Kim,⁶ B. R. Ko,¹⁷ S. Korpar,^{21,15} P. Križan,^{20,15} P. Krokovny,⁹ S.-H. Kyeong,⁴⁷ J. S. Lange,⁵ M. J. Lee,³⁸ S. E. Lee,³⁸ T. Lesiak,^{3,28} J. Li,⁸ A. Limosani,²² Y. Liu,²³ D. Liventsev,¹⁴ R. Louvot,¹⁹ A. Matyja,²⁸ S. McOnie,⁴⁰ H. Miyata,³⁰ Y. Miyazaki,²³ R. Mizuk,¹⁴ Y. Nagasaka,¹⁰ E. Nakano,³³ M. Nakao,⁹ H. Nakazawa,²⁵ Z. Natkaniec,²⁸ S. Nishida,⁹ K. Nishimura,⁸ O. Nitoh,⁴⁵ S. Ogawa,⁴¹ T. Ohshima,²³ S. Okuno,¹⁶ H. Ozaki,⁹ P. Pakhlov,¹⁴ G. Pakhlova,¹⁴ C. W. Park,³⁹ H. Park,¹⁸ H. K. Park,¹⁸ K. S. Park,³⁹ R. Pestotnik,¹⁵ L. E. Piilonen,⁴⁶ H. Sahoo,⁸ K. Sakai,³⁰ Y. Sakai,⁹ O. Schneider,¹⁹ J. Schümann,⁹ R. Seidl,³⁵ A. Sekiya,²⁴ K. Senyo,²³ M. E. Sevier,²² M. Shapkin,¹³ C. P. Shen,⁸ J.-G. Shiu,²⁷ B. Shwartz,^{1,32} A. Sokolov,¹³ S. Stanič,³¹ M. Starič,¹⁵ T. Sumiyoshi,⁴⁴ M. Tanaka,⁹ G. N. Taylor,²² Y. Teramoto,³³ S. Uehara,⁹ T. Uglov,¹⁴ Y. Unno,⁷ S. Uno,⁹ Y. Usov,^{1,32} G. Varner,⁸ K. E. Varvell,⁴⁰ K. Vervink,¹⁹ C. C. Wang,²⁷ C. H. Wang,²⁶ P. Wang,¹¹ X. L. Wang,¹¹ Y. Watanabe,¹⁶ R. Wedd,²² E. Won,¹⁷ B. D. Yabsley,⁴⁰ Y. Yamashita,²⁹ M. Yamauchi,⁹ C. Z. Yuan,¹¹ C. C. Zhang,¹¹ T. Zivko,¹⁵ A. Zupanc,¹⁵ and O. Zyukova^{1,32}

(Belle Collaboration)

¹*Budker Institute of Nuclear Physics, Novosibirsk*²*University of Cincinnati, Cincinnati, Ohio 45221*³*Kościuszko Cracow University of Technology, Krakow*⁴*Department of Physics, Fu Jen Catholic University, Taipei*⁵*Justus-Liebig-Universität Gießen, Gießen*⁶*The Graduate University for Advanced Studies, Hayama*⁷*Hanyang University, Seoul*⁸*University of Hawaii, Honolulu, Hawaii 96822*⁹*High Energy Accelerator Research Organization (KEK), Tsukuba*¹⁰*Hiroshima Institute of Technology, Hiroshima*¹¹*Institute of High Energy Physics, Chinese Academy of Sciences, Beijing*¹²*Institute of High Energy Physics, Vienna*¹³*Institute of High Energy Physics, Protvino*¹⁴*Institute for Theoretical and Experimental Physics, Moscow*¹⁵*J. Stefan Institute, Ljubljana*¹⁶*Kanagawa University, Yokohama*¹⁷*Korea University, Seoul*¹⁸*Kyungpook National University, Taegu*¹⁹*École Polytechnique Fédérale de Lausanne (EPFL), Lausanne*²⁰*Faculty of Mathematics and Physics, University of Ljubljana, Ljubljana*²¹*University of Maribor, Maribor*²²*University of Melbourne, School of Physics, Victoria 3010*²³*Nagoya University, Nagoya*²⁴*Nara Women's University, Nara*²⁵*National Central University, Chung-li*²⁶*National United University, Miao Li*²⁷*Department of Physics, National Taiwan University, Taipei*²⁸*H. Niewodniczanski Institute of Nuclear Physics, Krakow*²⁹*Nippon Dental University, Niigata*³⁰*Niigata University, Niigata*³¹*University of Nova Gorica, Nova Gorica*³²*Novosibirsk State University, Novosibirsk*³³*Osaka City University, Osaka*³⁴*Panjab University, Chandigarh*³⁵*RIKEN BNL Research Center, Upton, New York 11973*³⁶*Saga University, Saga*³⁷*University of Science and Technology of China, Hefei*

³⁸*Seoul National University, Seoul*³⁹*Sungkyunkwan University, Suwon*⁴⁰*University of Sydney, Sydney, New South Wales*⁴¹*Toho University, Funabashi*⁴²*Tohoku Gakuin University, Tagajo*⁴³*Department of Physics, University of Tokyo, Tokyo*⁴⁴*Tokyo Metropolitan University, Tokyo*⁴⁵*Tokyo University of Agriculture and Technology, Tokyo*⁴⁶*IPNAS, Virginia Polytechnic Institute and State University, Blacksburg, Virginia 24061*⁴⁷*Yonsei University, Seoul*

(Received 26 February 2009; published 30 April 2009)

We report on a search for the $X(1812)$ state in the decay $B^\pm \rightarrow K^\pm \omega \phi$ with a data sample of 657×10^6 $B\bar{B}$ pairs collected with the Belle detector at the KEKB e^+e^- collider. No significant signal is observed. An upper limit $\mathcal{B}(B^\pm \rightarrow K^\pm X(1812), X(1812) \rightarrow \omega \phi) < 3.2 \times 10^{-7}$ (90% C.L.) is determined. We also constrain the three-body decay branching fraction to be $\mathcal{B}(B^\pm \rightarrow K^\pm \omega \phi) < 1.9 \times 10^{-6}$ (90% C.L.).

DOI: 10.1103/PhysRevD.79.071102

PACS numbers: 12.39.Mk, 13.20.He

Using a sample of $5.8 \times 10^7 J/\psi$ events, the BES Collaboration observed a near-threshold enhancement in the $\omega \phi$ invariant mass spectrum from the double Okubo-Zweig-Iizuka (OZI) suppressed $J/\psi \rightarrow \gamma \omega \phi$ decay with a statistical significance of more than 10σ [1]. When fitted with a Breit-Wigner function, this enhancement, called $X(1812)$, has the following mass, width, and product of branching fractions:

$$M = (1812_{-26}^{+19} \pm 18) \text{ MeV}/c^2,$$

$$\Gamma = (105 \pm 20 \pm 28) \text{ MeV}/c^2,$$

$$\mathcal{B}(J/\psi \rightarrow \gamma X, X \rightarrow \omega \phi) = (2.60 \pm 0.27 \pm 0.65) \times 10^{-4}.$$

Partial wave analysis favors a spin-parity assignment of $J^{PC} = 0^{++}$ for the $X(1812)$. In the related $\omega \psi$ mode, Belle has seen a dramatic threshold enhancement in $B^+ \rightarrow K^+ \omega \psi$, the $Y(3940)$ [2], which has now been confirmed by BABAR [3].

If the $X(1812)$ is a $q\bar{q}$ meson, the $X(1812) \rightarrow \omega \phi$ branching fraction should be very small due to OZI suppression and the limited available phase space, in contrast with the BES observation. Suggestions have been made that the $X(1812)$ may be a tetraquark state (with structure $Q^2\bar{Q}^2$), since some tetraquark states decay to vector-vector mesons dominantly by “falling apart” and their masses are at the threshold of two vector mesons [4]. Other works speculate that it may be a hybrid [5], glueball state [6], an effect due to intermediate meson rescatterings [7] or a threshold cusp attracting a resonance [8]. In this paper, we report our search for this state in the decay $B^\pm \rightarrow K^\pm \omega \phi$. On the other hand, this decay proceeds via a $b \rightarrow s$ penguin with $s\bar{s}$ and $u\bar{u}$ popping. A similar decay mode $B^+ \rightarrow K^+ \phi \phi$, which proceeds via a $b \rightarrow s$ penguin diagram with double $s\bar{s}$ popping, is the only observed charmless $B \rightarrow VVP$ (two vector mesons and one pseudoscalar

meson) mode and has a rather large branching fraction $[(4.9_{-2.2}^{+2.4}) \times 10^{-6}]$ [9,10]. Therefore, even if the $X(1812)$ cannot be observed, measurement of the $B^\pm \rightarrow K^\pm \omega \phi$ three-body decay is also helpful for investigating decay mechanisms.

This analysis uses 605 fb^{-1} of data containing 657×10^6 $B\bar{B}$ pairs. The data was collected with the Belle detector [11] at the KEKB [12] e^+e^- asymmetric-energy (3.5 GeV on 8.0 GeV) collider operating at a center-of-mass (CM) energy of the $Y(4S)$ resonance.

The Belle detector is a large-solid-angle spectrometer [11]. It consists of a silicon vertex detector, a 50-layer central drift chamber (CDC), an array of aerogel threshold Cherenkov counters (ACC), time-of-flight scintillation counters (TOF), and an electromagnetic calorimeter comprised of CsI(Tl) crystals located inside a superconducting solenoid that provides a 1.5 T magnetic field. An iron flux return located outside the coil is instrumented to detect K_L^0 mesons and to identify muons (KLM).

B -daughter candidates are reconstructed from the decays $\omega \rightarrow \pi^+ \pi^- \pi^0$, $\phi \rightarrow K^+ K^-$, and $\pi^0 \rightarrow \gamma \gamma$. Charged tracks are identified as pions or kaons by combining information from the CDC, ACC and TOF systems. We reduce the number of poor quality tracks by requiring that $|dr| < 0.3 \text{ cm}$ and $|dz| < 1.5 \text{ cm}$, where $|dr|$ and $|dz|$ are the distances of closest approach of a track to the interaction point in the transverse plane and z direction (opposite to the direction of the positron beam), respectively. In addition, tracks matched with clusters in the electromagnetic calorimeter that are consistent with an electron hypothesis are rejected. We use a kaon identification likelihood ratio $R_{K,\pi} = L_K/(L_K + L_\pi)$ to discriminate K and π candidates. The requirements $R_{K,\pi} > 0.4$ for a kaon and $R_{K,\pi} < 0.6$ for a pion are used. The efficiency to identify a kaon (pion) is blue 94%(94%), while the probability that a pion (kaon) is misidentified as a kaon(pion) is about 11%(8%).

Candidate π^0 mesons are reconstructed from pairs of photons, where the energy of each photon in the laboratory frame is required to be greater than 50 MeV. We select π^0 mesons with an invariant mass in the range $0.1193 \text{ GeV}/c^2 < M(\gamma\gamma) < 0.1477 \text{ GeV}/c^2$ and a momentum in the laboratory frame $p_{\pi^0}^{\text{lab}} > 0.38 \text{ GeV}/c$.

Particles satisfying the above selection criteria are then used to reconstruct ω and ϕ mesons. We select candidates in the invariant mass windows $0.75 \text{ GeV}/c^2 < M_{\pi^+\pi^-\pi^0} < 0.81 \text{ GeV}/c^2$ and $1.00 \text{ GeV}/c^2 < M_{K^+K^-} < 1.04 \text{ GeV}/c^2$. A vertex fit and a mass-constrained fit for the ϕ and ω candidates are also performed. In addition, we require three kaons in the final state, one directly from the B -meson decay and the other two from the ϕ decay. To distinguish the two kinds of kaons and reduce multiple candidates, we require kaons from the ϕ to have momenta $p_{K^\pm} < 1.5 \text{ GeV}/c$ in the CM frame.

Candidate $B^\pm \rightarrow K^\pm \omega \phi$ decays are identified by using the energy difference (ΔE) and the beam-energy-constrained mass (M_{bc}). These are defined as $\Delta E \equiv E_B - E_{\text{beam}}$ and $M_{\text{bc}} \equiv \sqrt{E_{\text{beam}}^2 - p_B^2}$, where E_{beam} denotes the beam energy, E_B and p_B denote the reconstructed energy and momentum of the candidate B -meson, all evaluated in the e^+e^- CM frame. We select events satisfying $|\Delta E| < 0.2 \text{ GeV}$ and $5.20 \text{ GeV}/c^2 < M_{\text{bc}} < 5.29 \text{ GeV}/c^2$, and define signal regions $-0.15 \text{ GeV} < \Delta E < 0.05 \text{ GeV}$ and $5.27 \text{ GeV}/c^2 < M_{\text{bc}} < 5.29 \text{ GeV}/c^2$.

The dominant source of background arises from random combinations of particles in continuum $e^+e^- \rightarrow q\bar{q}$ events ($q = u, d, s, c$). To discriminate spherical $B\bar{B}$ events from jetlike $q\bar{q}$ events, we use event-shape variables: specifically, 16 modified Fox-Wolfram moments [13] combined into a Fisher discriminant, \mathcal{F} [14]. Additional discrimination is provided by θ_B , the polar angle in the CM frame between the B direction and z direction. Correctly reconstructed B mesons follow a $(1 - \cos^2\theta_B)$ distribution, while fake candidates from continuum tend to be uniform in $\cos\theta_B$.

Further continuum background suppression is achieved using b -flavor tagging information. The Belle flavor tagging algorithm [15] yields the flavor of the tagged meson,

$q (= \pm 1)$, and a flavor tagging quality factor, r . The latter ranges from zero for no flavor discrimination to one for unambiguous flavor assignment. For signal events, q is usually consistent with the flavor opposite to that of the signal B , while it is random for continuum events. Thus, the quantity qrF_B is used to separate signal and continuum events, where F_B is the charge of the signal B : $F_B = +1(-1)$ for B^+ (B^-).

We use a Monte Carlo (MC) sample [16] to form \mathcal{F} and to obtain the $\cos\theta_B$ and qrF_B distributions (shown in Fig. 1). Probability density functions (PDFs) are derived from \mathcal{F} and the $\cos\theta_B$ distributions and are multiplied to form signal (L_s) and continuum background ($L_{q\bar{q}}$) likelihood functions, which are further combined to form a likelihood ratio $R_s = L_s/(L_s + L_{q\bar{q}})$. We divide events into six qrF_B bins and determine the optimum R_s selection criteria for each bin by maximizing $N_s/\sqrt{N_s + N_b}$, where N_s is the number of signal MC events in the signal region, and N_b is the number of background MC events in the signal region estimated by assuming $\mathcal{B}(B^\pm \rightarrow K^\pm \omega \phi) = 1.0 \times 10^{-5}$. This optimization preserves 57.9% of the signal while rejecting 98.6% of the continuum background.

Applying all of the above criteria, the fraction of events having multiple candidates is 21%. To select the B -meson candidate, we add the χ^2 of the ω -meson vertex fit, and the χ^2 of a $\pi^0 \rightarrow \gamma\gamma$ fit constrained to the Particle Data Group (PDG) [17] value of π^0 mass: the candidate with the smallest value is chosen. If multiple B candidates still remain, we use the χ^2 of the ϕ meson vertex fit and χ^2 of the B -meson vertex fit to choose the best one.

In addition to the dominant continuum background, charmed B decay ($b \rightarrow c$) and charmless B decay ($b \rightarrow u, d, s$) backgrounds are studied using dedicated MC samples that are, respectively, about 2 and 25 times the size of the data sample. Charmless B decay background is found to be small and is neglected. The following charmed B decay channels are studied using dedicated Monte Carlo samples: $B^\pm \rightarrow D_s^\mp \pi^0 \pi^\pm K^\pm$, $D_s^\pm \rightarrow \pi^\pm \phi$; $B^\pm \rightarrow D_s^\mp \pi^\pm K^\pm$, $D_s^\pm \rightarrow \pi^0 \pi^\pm \phi$ and $B^\pm \rightarrow \bar{D}^0/D^0 K^\pm$, $D^0/\bar{D}^0 \rightarrow \pi^+ \pi^- \pi^0 K^+ K^-$. To measure the three-body $B^\pm \rightarrow K^\pm \omega \phi$ branching fraction, we require $M_{K^+K^- \pi^+ \pi^- \pi^0} > 2.2 \text{ GeV}/c^2$ to exclude D^0 background,

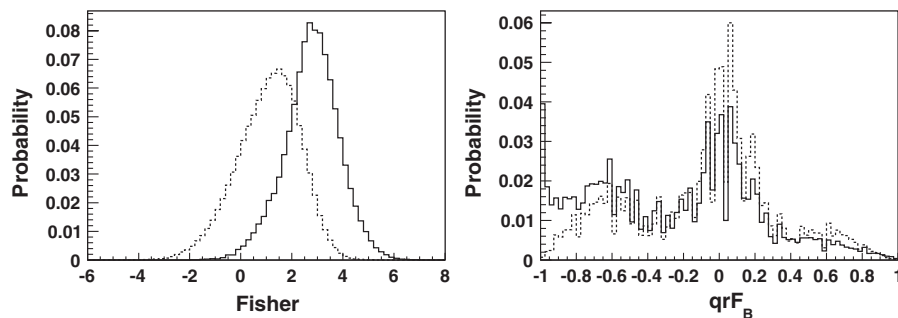


FIG. 1. Distribution of \mathcal{F} (left) and qrF_B (right): signal (dot-dashed line), $q\bar{q}$ (dashed line).

C. LIU *et al.*

and require $|M_{\pi K^+ K^-} - m_{D_s}| > 0.15 \text{ GeV}/c^2$ as well as $|M_{\pi^0 \pi^+ K^-} - m_{D_s}| > 0.15 \text{ GeV}/c^2$, where m_{D_s} is the nominal D_s mass [17], to veto the D_s background.

We obtain the signal yield using a four-dimensional extended unbinned maximum likelihood (ML) fit to ΔE , M_{bc} , $M_{\pi\pi\pi}$, and M_{KK} . The likelihood function consists of the following components: signal decays, continuum background ($q\bar{q}$), and charmed B -decay background ($b \rightarrow c$). For all components, no sizable correlations are found among the fitting quantities. The PDF for event i and component j is defined as

$$\mathcal{P}_j^i = \mathcal{P}_j(\Delta E^i) \times \mathcal{P}_j(M_{bc}^i) \times \mathcal{P}_j(M_{KK}^i) \times \mathcal{P}_j(M_{\pi\pi\pi}^i). \quad (1)$$

The signal M_{bc} is parametrized by the sum of a single Gaussian and an ARGUS function [18], ΔE by the sum of a Gaussian and a Crystal Ball function [19], and $M_{K^+ K^-}$, $M_{\pi^+ \pi^- \pi^0}$ by Breit-Wigner functions. For continuum background, M_{bc} is parametrized by an ARGUS function, ΔE by a second-order Chebyshev polynomial, and $M_{K^+ K^-}$, $M_{\pi^+ \pi^- \pi^0}$ by the sum of Breit-Wigner functions and first-order Chebyshev polynomials. $B\bar{B}$ background modeling is similar, but with a first-order Chebyshev for ΔE and for $M_{\pi^+ \pi^- \pi^0}$. All function parameters are determined from MC simulation.

The likelihood function to be maximized is given by

$$\mathcal{L} = \frac{e^{-(\sum_j Y_j)}}{N!} \prod_{i=1}^N \sum_j (Y_j \mathcal{P}_j^i), \quad (2)$$

where Y_j is the yield of events for component j and N is the total number of events in the sample.

In the unbinned four-dimensional fit, the signal, and $q\bar{q}$ yields are allowed to vary; the fraction of $b \rightarrow c$ events is very small and thus its yield is fixed according to MC.

After using samples of MC simulation to validate our fitting procedure, we apply the fit to the data. Figure 2 shows the fit results. Peaking behavior observed in ΔE , M_{bc} , $M_{\pi\pi\pi}$, and M_{KK} is consistent with that from MC expectations. The branching fraction is evaluated using the following quantities: the signal yield $Y_{\omega\phi K} = 22.1^{+8.3}_{-7.2}$ with reconstruction efficiency $\varepsilon = 7.04 \times 10^{-2}$; the combined daughter branching fraction $\mathcal{B}_d = 0.439$ [17]; a correction of 0.946 to the efficiency of K/π identification requirements, which takes into account small differences between MC and data; and a total of 657×10^6 produced $B\bar{B}$ pairs, where equal fractions of $B^+ B^-$ and $B^0 \bar{B}^0$ are assumed.

The sources of systematic error are listed in Table I. The quoted 6% track reconstruction efficiency is from the

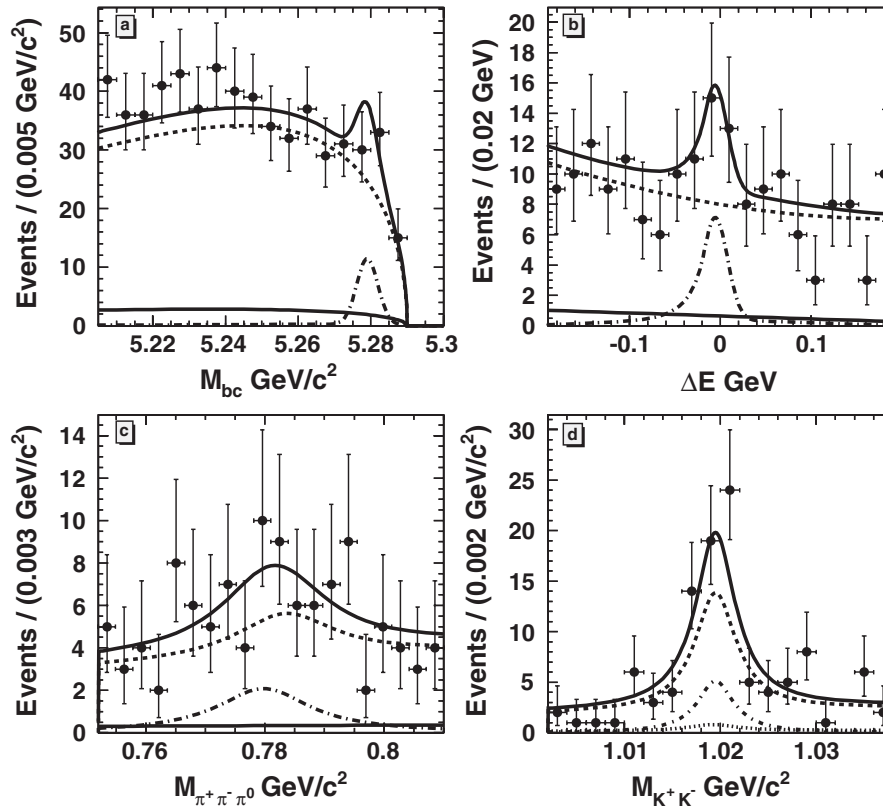


FIG. 2. Projection of the data (points with error bars) and fit results onto (a) M_{bc} , (b) ΔE , (c) $M_{\pi^+ \pi^- \pi^0}$, (d) $M_{K^+ K^-}$ with the other variables satisfying $M_{bc} \in (5.27, 5.29) \text{ GeV}/c^2$, $\Delta E \in (-0.15, 0.05) \text{ GeV}$, $M_{\pi^+ \pi^- \pi^0} \in (-0.75, 0.81) \text{ GeV}/c^2$, $M_{K^+ K^-} \in (1.00, 1.04) \text{ GeV}/c^2$: signal (dot-dashed line), $q\bar{q}$ (dashed line), $B\bar{B}$ (dot-dot-dot-dashed line) and total (solid line).

SEARCH FOR THE $X(1812)$ IN ...

TABLE I. Systematic errors for $\mathcal{B}(B^\pm \rightarrow K^\pm \omega \phi)$. In cases where the error on $\mathcal{B}(B^\pm \rightarrow K^\pm X, (1812), X(1812) \rightarrow \omega \phi)$ is different, it is shown separately in parentheses.

Type	Fractional error (%)	
	$+\sigma$	$-\sigma$
Tracking	6.00	6.00
K/π ID	2.90	2.90
π^0 reconstruction	4.00	4.00
Daughter \mathcal{B}	1.45	1.45
Signal/background modeling	5.25(31.1)	2.50(22.7)
$B\bar{B}$ Background yield	1.75(2.10)	0.89(1.60)
MC statistics	0.56(1.06)	0.56(1.06)
Continuum suppression	7.21(12.0)	7.26(12.4)
$N_{B\bar{B}}$	1.36(1.36)	1.36(1.36)
Total	12.1(34.4)	11.2(27.1)

consideration that there are five tracks in a selected event and for each track the efficiency error is 1.2%. The errors due to continuum suppression requirements are obtained by varying these cuts while the errors on the PDF shapes are obtained by varying all fixed parameters by $\pm 1\sigma$. Toy MC tests and GEANT-based detector simulation tests are performed, we find that the fit bias can be neglected. To estimate the error due to the $b \rightarrow c$ contribution, we vary the normalizations by $\pm 50\%$.

Our final result for the three-body branching fraction based on the 605 fb^{-1} data sample is

$$\mathcal{B}(B^\pm \rightarrow K^\pm \omega \phi) = (1.15^{+0.43+0.14}_{-0.38-0.13}) \times 10^{-6},$$

where the first error quoted is statistical and the second systematic. We obtain the 90% confidence level upper limit $\mathcal{B}(B^\pm \rightarrow K^\pm \omega \phi) < 1.9 \times 10^{-6}$ by a frequentist method using ensembles of pseudoexperiments. For a given signal yield, 10000 sets of signal and background events are generated according to the PDFs, and fits are performed. The confidence level is obtained from the fraction of samples that gives a fit yield larger than that of data (22.1). We take into account systematic errors by varying the fit yield by the total systematic errors described in Table I. The significance of the signal, estimated using this method, is 2.8σ .

We next study the $\omega \phi$ mass spectrum. Because the aforementioned $M_{K^+K^-\pi^+\pi^-\pi^0}$, $|M_{\pi K^+K^-} - m_{D_s}|$ and $|M_{\pi^0\pi K^+K^-} - m_{D_s}|$ mass cuts influence the shape of the $\omega \phi$ invariant mass spectrum, we did not use them and fit the D^0 and D_s backgrounds simultaneously.

We produced 0.6×10^6 (2.0×10^6) D^0 (D_s) background MC events for the decay $B^\pm \rightarrow K^\pm X(1812), X(1812) \rightarrow \omega \phi$. The $X(1812)$ mass and width are taken from the BES measurement and its PDF is modeled by a reversed ARGUS (rARGUS) [18], $F_{\text{rARGUS}}(x) = F_{\text{ARGUS}}(2t - x)$, where t is the threshold) function plus a Breit-Wigner with a threshold. The three-body decay PDF is an rARGUS function, the D^0 background PDF is the sum of

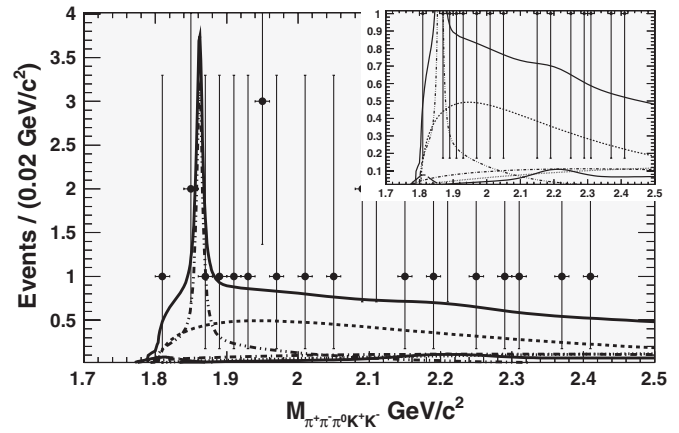


FIG. 3. Mass spectrum in the $\omega \phi$ fit with the following components: $B^+ \rightarrow K \omega \phi$ three-body (dotted line), $B\bar{B}$ (dot-dashed line), $q\bar{q}$ (dashed), D^0 (dot-dot-dashed line), D_s (dot-dot-dot-dashed line), $B^\pm \rightarrow K^\pm X(1812)$ (long-dashed line), and total (solid line). The spectrum is also shown in the inset with an expanded vertical scale.

an rARGUS function and a Breit-Wigner function, the D_s background is the sum of an rARGUS function and a Gaussian function, while the $q\bar{q}$, $B\bar{B}$ backgrounds are also modeled by rARGUS functions. We obtained all the parameters from MC samples. In our final unbinned fit to the data, we fixed the yield of D^0 and D_s backgrounds according to the PDG branching fractions [17], and fixed the yield of $B\bar{B}$ background according to MC simulation.

The final result is shown in Fig. 3. No significant signal is observed; the yield of the $X(1812)$ is $0.2^{+2.4}_{-1.5}$ events. The systematic errors are also listed in Table I, where those in parentheses are for the items that differ from those in the three-body decay analysis. We also include the errors from the fraction of D^0 , D_s background and the $X(1812)$ width into signal/background modeling. Using the pseudoexperiment method described above and taking the systematic errors into account, we find a limit on the product branching fraction of $\mathcal{B}(B^\pm \rightarrow K^\pm X(1812), X(1812) \rightarrow \omega \phi) < 3.2 \times 10^{-7}$ (90% C.L.)

In summary, using a data sample of 605 fb^{-1} collected with the Belle detector, we present a search for the $X(1812)$ meson in the decay $B^\pm \rightarrow K^\pm \omega \phi$. No significant signal is observed. An upper limit for the product $\mathcal{B}(B^\pm \rightarrow K^\pm X(1812), X(1812) \rightarrow \omega \phi) < 3.2 \times 10^{-7}$ (90% C.L.) is determined. We also measure the three-body $B^\pm \rightarrow K^\pm \omega \phi$ decay branching fraction $\mathcal{B}(B^\pm \rightarrow K^\pm \omega \phi) = [1.15^{+0.43+0.14}_{-0.38-0.13} (< 1.9)] \times 10^{-6}$, where the upper limit is at the 90% confidence level.

We thank the KEKB group for the excellent operation of the accelerator, the KEK cryogenics group for the efficient operation of the solenoid, and the KEK computer group and the National Institute of Informatics for valuable computing and SINET3 network support. We acknowledge support from the Ministry of Education, Culture, Sports,

Science, and Technology (MEXT) of Japan, the Japan Society for the Promotion of Science (JSPS), and the Tau-Lepton Physics Research Center of Nagoya University; the Australian Research Council and the Australian Department of Industry, Innovation, Science and Research; the National Natural Science Foundation of China under Contract Nos. 10575109, 10775142, 10875115, and 10825524; the Department of Science and Technology of India; the BK21 program of the Ministry of Education of Korea, the CHEP source code program and Basic Research program (Grant No. R01-2008-000-10477-0) of the Korea Science and Engineering Foundation; the

Polish Ministry of Science and Higher Education; the Ministry of Education and Science of the Russian Federation and the Russian Federal Agency for Atomic Energy; the Slovenian Research Agency; the Swiss National Science Foundation; the National Science Council and the Ministry of Education of Taiwan; and the U.S. Department of Energy. This work is supported by a Grant-in-Aid from MEXT for Science Research in a Priority Area (“New Development of Flavor Physics”), and from JSPS for Creative Scientific Research (“Evolution of Tau-lepton Physics”).

-
- [1] M. Ablikim *et al.* (BES Collaboration), Phys. Rev. Lett. **96**, 162002 (2006).
- [2] K. Abe *et al.* (Belle Collaboration), Phys. Rev. Lett. **94**, 182002 (2005).
- [3] B. Aubert *et al.* (BABAR Collaboration), Phys. Rev. Lett. **101**, 082001 (2008).
- [4] B. A. Li, Phys. Rev. D **74**, 054017 (2006).
- [5] K. T. Chao, arXiv:hep-ph/0602190.
- [6] P. Bicudo, S. R. Cotanch, F. J. Llanes-Estrada, and D. G. Robertson, Eur. Phys. J. C **52**, 363 (2007).
- [7] Q. Zhao and B. S. Zou, Phys. Rev. D **74**, 114025 (2006).
- [8] D. V. Bugg, J. Phys. G **35**, 075005 (2008).
- [9] K. Abe *et al.* (Belle Collaboration), arXiv:hep-ex/0802.1547.
- [10] B. Aubert *et al.* (BABAR Collaboration), Phys. Rev. Lett. **97**, 261803 (2006).
- [11] A. Abashian *et al.* (Belle Collaboration), Nucl. Instrum. Methods Phys. Res., Sect. A **479**, 117 (2002).
- [12] S. Kurokawa and E. Kikutani, Nucl. Instrum. Methods Phys. Res., Sect. A **499**, 1 (2003), and other papers included in this volume.
- [13] S. H. Lee *et al.* (Belle Collaboration), Phys. Rev. Lett. **91**, 261801 (2003).
- [14] G. C. Fox and S. Wolfram, Phys. Rev. Lett. **41**, 1581 (1978).
- [15] H. Kakuno *et al.*, Nucl. Instrum. Methods Phys. Res., Sect. A **533**, 516 (2004).
- [16] For the EVTGEN generator, see: D. J. Lange, Nucl. Instrum. Methods Phys. Res., Sect. A **462**, 152 (2001); The detector response is simulated with GEANT, R. Brun *et al.*, CERN Report No. DD/EE/84-1, 1984.
- [17] C. Amisler *et al.* (Particle Data Group), Phys. Lett. B **667**, 1 (2008).
- [18] H. Albrecht *et al.* (ARGUS Collaboration), Phys. Lett. B **241**, 278 (1990).
- [19] T. Skwarnicki, Ph.D. thesis, Institute for Nuclear Physics, Krakow, 1986; DESY Report No. DESY F31-86-02, 1986 (unpublished).